AFRL-RZ-WP-TP-2010-2251

FUEL/AIR MIXING CHARACTERISTICS OF STRUT INJECTIONS FOR SCRAMJET COMBUSTOR APPLICATIONS (POSTPRINT)

Chung-Jen Tam

Taitech, Inc.

Kuang-Yu Hsu

Innovative Scientific Solutions, Inc.

Mark R. Gruber and Charbel N. Raffoul

Aerospace Propulsion Division

AUGUST 2008

AIR FORCE RESEARCH LABORATORY
PROPULSION DIRECTORATE
WRIGHT-PATTERSON AIR FORCE BASE, OH 45433-7251
AIR FORCE MATERIEL COMMAND
UNITED STATES AIR FORCE

REPORT DOCUMENTATION PAGE

Form Approved
OMB No. 0704-0188

1. REPORT DATE *(DD-MM-YY)*	2. REPORT TYPE	3. DATES COVERED *(From - To)*
August 2008	Conference Paper Postprint	01 August 2007 – 18 August 2008

4. TITLE AND SUBTITLE
FUEL/AIR MIXING CHARACTERISTICS OF STRUT INJECTIONS FOR SCRAMJET COMBUSTOR APPLICATIONS (POSTPRINT)

5a. CONTRACT NUMBER
In-house

5b. GRANT NUMBER

5c. PROGRAM ELEMENT NUMBER
62203F

6. AUTHOR(S)
Chung-Jen Tam (Taitech, Inc.)
Kuang-Yu Hsu (Innovative Scientific Solutions, Inc.)
Mark R. Gruber (AFRL/RZAS)
Charbel N. Raffoul (AFRL/RZAT)

5d. PROJECT NUMBER
3012

5e. TASK NUMBER
AI

5f. WORK UNIT NUMBER
3012AI00

7. PERFORMING ORGANIZATION NAME(S) AND ADDRESS(ES)
Taitech, Inc.
Beavercreek, OH 45430

Innovative Scientific Solutions, Inc.
Dayton, OH 45440

Propulsion Sciences Branch (AFRL/RZAS)
Propulsion Technology Branch (AFRL/RZAT)
Aerospace Propulsion Division
Air Force Research Laboratory, Propulsion Directorate
Wright-Patterson Air Force Base, OH 45433-7251
Air Force Materiel Command, United States Air Force

8. PERFORMING ORGANIZATION REPORT NUMBER
AFRL-RZ-WP-TP-2010-2251

9. SPONSORING/MONITORING AGENCY NAME(S) AND ADDRESS(ES)
Air Force Research Laboratory
Propulsion Directorate
Wright-Patterson Air Force Base, OH 45433-7251
Air Force Materiel Command
United States Air Force

10. SPONSORING/MONITORING AGENCY ACRONYM(S)
AFRL/RZAS

11. SPONSORING/MONITORING AGENCY REPORT NUMBER(S)
AFRL-RZ-WP-TP-2010-2251

12. DISTRIBUTION/AVAILABILITY STATEMENT
Approved for public release; distribution unlimited.

13. SUPPLEMENTARY NOTES
Conference paper published in the *Proceedings of the 26th AIAA Applied Aerodynamics Conference*, conference held 18 - 21 August 2008 in Honolulu, HI. This paper contains color. PA Case Number: WPAFB 08-4808; Clearance Date: 18 Jul 2008.

14. ABSTRACT
Numerical studies were performed to determine the fuel/air mixing characteristics of several strut fuel-injection schemes for possible use in round scramjet-combustor applications. Gaseous ethylene was used as the fuel injectant. A total of fourteen strut-injection schemes were conducted with a Mach 2 inflow condition in a rectangular flow path. In addition, the StrutE-s-2 design was simulated in a Mach 3 flow to provide a better understanding of fuel/air mixing capability under various flow conditions. The fuel ports were placed in various locations on the struts, including the leading edge, side, tip and wall. The performance of these strut-injection designs is determined based on the local equivalence ratio, total pressure recovery, and mixing efficiency in a rectangular flow path. Most of the strut designs have a backward-swept angle, except Strut J, which has a forward-swept angle. In general, the backward-swept strut transports the fuel upward toward the core flow. On the other hand, a forward-swept strut carries the fuel toward the bottom wall. Numerical results indicate that StrutE-les-1 has the best performance.

15. SUBJECT TERMS
supersonic combustion, strut injection, CFD

16. SECURITY CLASSIFICATION OF:			17. LIMITATION OF ABSTRACT:	18. NUMBER OF PAGES	19a. NAME OF RESPONSIBLE PERSON (Monitor)
a. REPORT	b. ABSTRACT	c. THIS PAGE			Mark R. Gruber
Unclassified	Unclassified	Unclassified	SAR	22	19b. TELEPHONE NUMBER *(Include Area Code)* N/A

Standard Form 298 (Rev. 8-98)
Prescribed by ANSI Std. Z39-18

26th AIAA Applied Aerodynamics Conference
18 - 21 August 2008, Honolulu, Hawaii

AIAA 2008-6925

Fuel/Air Mixing Characteristics of Strut Injections for Scramjet Combustor Applications

Chung-Jen Tam[¶]
Taitech, Inc., Beavercreek, OH 45430

Kuang-Yu Hsu[§]
Innovative Scientific Solutions, Inc., Dayton, OH 45440

Mark R. Gruber[†]
AFRL/RZAS, Wright-Patterson Air Force Base, OH 45433

and

Charbel N. Raffoul[‡]
AFRL/RZAT, Wright-Patterson Air Force Base, OH 45433

Numerical studies were performed to determine the fuel/air mixing characteristics of several strut fuel-injection schemes for possible use in round scramjet-combustor applications. Gaseous ethylene was used as the fuel injectant. A total of fourteen strut-injection schemes were conducted with a Mach 2 inflow condition in a rectangular flow path. In addition, the StrutE-s-2 design was simulated in a Mach 3 flow to provide a better understanding of fuel/air mixing capability under various flow conditions. The fuel ports were placed in various locations on the struts, including the leading edge, side, tip and wall. The performance of these strut-injection designs is determined based on the local equivalence ratio, total pressure recovery, and mixing efficiency in a rectangular flow path. Most of the strut designs have a backward-swept angle, except Strut J, which has a forward-swept angle. In general, the backward-swept strut transports the fuel upward toward the core flow. On the other hand, a forward-swept strut carries the fuel toward the bottom wall. The numerical result indicates that StrutE-les-1 has the best performance in terms of overall total pressure recovery and mixing efficiency. These computations will be followed by an experimental program to assess mixing, pressure loss, and general flowfield characteristics.

Nomenclature

H	=	strut height	T_0	=	total temperature at the facility nozzle
L	=	strut length	W	=	half-strut width
M	=	Mach number	x	=	streamwise direction
P_0	=	total pressure at the facility nozzle	y^+	=	yv^*/v
RC	=	research cell	y	=	normal direction
φ	=	equivalence ratio			

I. Introduction

One of the principal challenges in developing large-scale scramjet-engine designs is the fuel-injection strategy, *i.e.*, the penetration and mixing of the fuel in the combustor. Injector designs must effectively enhance fuel penetration into the core flow to produce rapid mixing and combustion of fuel and air without excessive increase in jet-injection supply pressure. In addition, injector designs and the flow disturbances produced by injection should

¶ Sr. Research Scientist, Taitech Inc., 1430 Oak Court, Suite 301, Beavercreek, OH 45430, Associate Fellow AIAA.
§ Sr. Research Scientist, ISSI., 2766 Indian Ripple Road, Dayton, OH 45440, Associate Fellow AIAA.
† Sr. Aerospace Engineer, AFRL/RZAS, WPAFB, OH 45433, Associate Fellow AIAA.
‡ Program Manager, AFRL/RZAT, WPAFB, OH 45433.

provide a region for flame holding, and thus a stable piloting source for downstream ignition of the fuel, without introducing excessive total pressure losses. Jet-injection designs for scramjet-engine applications can be divided into two categories: non-intrusive and intrusive fuel jet injection technologies. The non-intrusive designs include primarily flush-wall injectors, which minimize the total pressure loss. These injectors can be classified by angle (normal, low-angled, and transverse),[1-4] shape (circular, elliptical, wedge, and diamond shaped),[5-8] and configuration (aeroramp, cascade, and swirl injectors).[9-16]

Intrusive concepts for fuel mixing enhancement include ramps, pylons, and struts.[17-21] These designs tend to create more aerodynamic disturbances than non-intrusive mechanisms, with an inevitable increase in total pressure losses and drag. Active cooling, with its associated complexities, is usually required for intrusive devices. Nevertheless, such designs do, in general, provide better fuel-air mixing in the scramjet combustor, and they could potentially enhance the combustion process, significantly reducing the required length of the scramjet engine. These benefits may well be great enough to outweigh the drawbacks.

The present research focuses on the use of a strut-injection technique for a large-scale round scramjet combustor. Struts offer the possibility of injecting fuel directly into the core of a supersonic flow without using high fuel supply pressure. On the other hand, since the strut is exposed to the main flow, the total pressure losses, heat flux and flow disturbance must be evaluated as part of the design process. Numerical studies were performed in a pre-test analysis of different fuel-injector strategies for better mixing flow features for round scramjet-combustor applications. The mixing characteristics of several fueling schemes were examined using gaseous ethylene. The conceptual single-strut designs were studied in a rectangular flow path, because the computations will be evaluated experimentally in the AFRL/RZA Research Cell 19 supersonic wind-tunnel facility at Wright-Patterson Air Force Base, OH, which has a rectangular cross-section area of 12.7 *cm* x 15.24 *cm*.

II. Numerical Approach

All simulations were performed using the CFD^{++} code, a general-purpose CFD tool developed by Metacomp Technologies.[22] CFD^{++} uses a finite-volume numerical framework, with multi-dimensional TVD schemes and Riemann solvers for accurate representation of supersonic flows. Several types of Riemann solver are available; the HLLC Riemann solver with minmod flux limiting was used in the simulations described here. Multi-grid acceleration is available to provide a fast and accurate solution methodology for both steady and unsteady flows. A variety of one-, two-, and three-equation turbulence models are available for RANS calculations, along with large eddy simulation (LES) and hybrid RANS/LES options. Unless otherwise specified, turbulence was modeled using the two-equation cubic κ-ε model. This model has non-linear terms that account for normal-stress anisotropy, swirl and streamline curvature effects. At solid surfaces, an advanced two-layer wall function with equilibrium and non-equilibrium blending was employed to reduce grid requirements. Chemically reacting flows can be modeled with general finite-rate kinetics models. The code supports both structured (quadrilateral and hexahedral) and unstructured (triangle, prism, and tetrahedral) grids. An MPI is used to take advantage of modern parallel-processing computers. The numerical solutions were considered to be converged based on the residual history and the steadiness of the mass flow rate. The mass flow rate should not change, that is, it should be constant along the entire length of the isolator.

The mixing efficiency is defined as follows:

$$\eta_m = \frac{\int Y_r \rho(\vec{v}\cdot\vec{n})\,dA}{\int Y \rho(\vec{v}\cdot\vec{n})\,dA}$$

where Y is the mass fraction of the lean constituent (based on the global equivalence ratio) and Y_r is the mass fraction of the least available reactant that would react if complete reaction were to take place without further mixing, *i.e.*,

$$Y_r = \begin{cases} Y, & Y \le Y_s \\ \left(\dfrac{1-Y}{1-Y_s}\right) Y_s, & Y > Y_s \end{cases}$$

The definition of perfect mixing implied by this measure requires that the least available reaction (Y) be less than or equal to the stoichiometric value (Y_s) at every point of a given streamwise plane.

Initial/Boundary Conditions and Grid

The conceptual strut configurations were simulated with inflow conditions of M = 2 and 3 with T_0 = 294 *K* and P_0 = 344.7 *kPa*, which correspond to the test conditions available in the AFRL/RZA RC 19 facility.[23] The

supersonic wind tunnel is a direct-connect facility (that is, the test section is connected to the exit of the facility nozzle). The RC 19 test section has a cross-sectional area of 12.7 *cm* x 15.24 *cm* (5″ x 6″), with a length of 63.5 *cm* (25″). The numerical simulations were extended from the facility nozzle plenum to the entrance of the test section to provide the inflow conditions for the test section, as illustrated in Figure 1. This practice obviates the use of ad-hoc profiles at the test section entrance. A no-slip, adiabatic boundary condition was imposed on the solid walls and the strut surfaces. A zero-gradient condition was applied at the outflow plane. Centerline symmetry was assumed, so only half of the strut configuration was computed for most of the cases in this study, as depicted in Figure 2. In two cases, however, the strut is asymmetric and has a flat surface on one side; in these cases the whole cross-sectional area was included in the computational domain.

Gaseous ethylene fuel was used as the injectant in these simulations, with a total mass flow rate of 1.9634×10^{-3} *kg*/*sec*, with the fuel flow rate equally divided among the injector ports. The diameter of each injector is 0.01016 *cm* (0.04″). Note that the ethylene-fuel inflow conditions were set up as a boundary condition on the strut surfaces. Thus, no computational grid was created for the injector port. The computational domains consisted of 2.6 million grid cells. The grid was clustered to all solid surfaces at a level appropriate for the use of wall functions ($y^+ \leq 70$). Although CFD^{++} allows unstructured grids, a structured-grid topology was used to provide better constant grid clusterings without significantly increasing the number of grid cells.

Fuel-port arrangements

Fourteen fuel-injector port configurations were tested numerically to determine their performance, based on total pressure recovery and mixing characteristics. The baseline strut design, StrutE, was chosen based on previous numerical results.[24] Among the six different strut conceptual designs tested earlier, this configuration was found to offer relatively good mixing capability, based on the vorticity contours and streamline flow features, without a significant total pressure recovery penalty. The length (*L*), height (*H*) and width (*W*) of this strut are 5.08 *cm* (2″), 2.54 *cm* (1″), and 0.4763 *cm* (3/16″), respectively, as illustrated in Figure 2. Note that the total width of the strut is actually 0.9525 *cm* (3/8″), but only half of the strut is simulated, as mentioned earlier.

For ten of the cases, 6 fuel injector ports were placed on the leading edge and/or sides of the strut, with three on each side of the center line or symmetry plane, as shown in Figure 3a-e, Figure 4, and Figure 5b. The injector port arrangements for these fuel mixing studies are listed in Table 1. Note that the notations for the fuel ports are listed below Table 1. For StrutE-st, StrutE-sw-1, StrutE-sw-2, and StrutI-les-1, the fuel port configuration is slightly different. StrutE-st has three injector ports on each side and one on tip of the strut (Figure 3f), with a total of seven fuel ports in this design. StrutE-sw-1 and StrutE-sw-2 have a flush-wall injector on the bottom wall, which is located on the mid-span of the leading edge and side of the strut, respectively, with its center located 0.1016 *cm* (0.04") from the strut surface, as illustrated in (Figure 3g and Figure 3h). In these designs, there are only four fuel ports on the strut. The flush-wall-injector design is based on the flow structures observed in the previous numerical study.[24] The flow near the strut surface tends to turn upward after the leading edge due to the sweep angle and the low pressure region along the sidewall of the strut. Fuel from a flush-wall injector close to the strut surface could potentially be transported upward toward the tip of the strut. In addition, this design would permit a simpler fuel flow path within the strut, because there are two fewer fuel ports on the strut (Table 1). For StrutI-les-1 configuration, there are only three injector ports on the strut surface (Figure 5a). On the other hand, the StrutI-les-2 design has three more ports located on the flat surface of the strut, on the opposite side (Figure 5b). These two configurations have an asymmetric strut design and are only half as wide as the other designs. Hence, the full isolator cross-section area was computed for these two cases. Most of the strut designs have a backward-swept angle, except for Strut-J which has a forward-swept strut, as shown in Figure 6.

In all cases, the second and third injectors are 1.27 *cm* (0.50*H*) and 1.905 *cm* (0.75*H*) away from the bottom wall. The location of the first injector is 0.635 *cm* (0.25*H*) away from the bottom wall (Figure 3b), except for StrutE-le-2, StrutE-s-2, StrutH-les, StrutI-les-1, and StrutI-les-2, on which it is 0.3175 *cm* (0.12*H*) from the wall (Figure 3d). Note that all the injectors are located either on the mid-span of the leading edge or on the side surfaces, with the exception of StrutE-sw-1 and StrutE-sw-2, as discussed above.

III. Results

Fuel/air mixing studies for various strut configurations were simulated with inflow conditions of $M = 2$ with $T_0 = 294\ K$ and $P_0 = 344.7\ kPa$. In addition, for the StrutE-s-2 design, a simulation was also performed for Mach 3 with the same total conditions, to provide a comparison in mixing efficiency at different flight conditions. Note that the mass flow rate of gaseous ethylene is 1.9634×10^{-3} *kg*/*sec* ($\varphi = 3.1 \times 10^{-3}$), which is consistent with earlier

experimental work on cavity-strut combustion.[25] The emphasis of the present fuel/air mixing studies is on the vicinity of the strut region, to understand the mixing flow characteristics without the effect of the reflected shock wave from the walls of the wind tunnel downstream of the strut. In addition, this study was intended to mimic a section of an eight-strut configuration in a round combustor, as depicted in Figure 7.[24] The amount of fuel injected from the strut is therefore kept relatively small to minimize the flow disturbance from adjacent struts.

The results are presented in terms of the flow field data and 1-D mass-averaged quantities to depict the fuel distributions in the vicinity of the strut, and the effects of the various fueling schemes and strut designs on performance. The flow field data are presented in terms of static pressure and equivalence ratio contours, and the 1-D analysis is represented by total pressure recovery and mixing efficiency.

Figure 8 - Figure 17 show pressure and equivalence ratio contours for the various fueling schemes and variations on the StrutE designs. The contours on the cross-section planes, *ie.*, x = 0.9398, 0.9652, 0.9906 and 1.016 *m*, are the equivalence ratios at locations 2.54 *cm* (1.0") apart in the streamwise direction. The static pressure contours are on the symmetry plane or side wall (StrutI-les-1 and StrutI-les-2), bottom wall and strut surfaces. Note that both legends are included in the figures. All the numerical results are for simulated Mach 2 flow conditions, except for Figure 17, which shows a Mach 3 simulation using the StrutE-s-2 configuration.

StrutE with various fueling schemes

Figure 8 shows the fueling schemes for the StrutE configuration. Overall, there are no significant differences in the penetration height of the fuel plume behind the strut (x = 1.016 *m*), even for the StrutE-st case (Figure 8f). Although the StrutE-st design has a fuel injector on the tip of the strut, the fuel is pushed downward at the trailing edge of the strut by the flow around the expansion corner. Thus, this design does not provide significantly more fuel penetration to the core flow than do other fueling schemes. The other flow feature to be considered is the lateral spreading of the fuel plume, and particularly the fuel concentration near the bottom wall, because of the necessity of coupling the fuel injection and the ignition source. In general, the ignition source would be placed behind the strut and flush with the bottom wall. Therefore, there must be sufficient fuel near the ignition source to provide successful combustion. Placing the first injector port at the leading edge of the strut and close to the bottom wall (1/8 *H*), as in the case of StrutE-le-2 and StrutE-les-1 (Figure 8c and Figure 8e), seems to improve the fuel concentration near the bottom wall as compared to other fueling schemes (Figure 8), particularly at x = 0.9398 *m*. This improvement is mainly due to the injection of fuel in the low momentum region or close to the bottom wall. For instance, the only difference between StrutE-le-1 and StrutE-le-2 designs is the placement of the first fuel port, which is 1/4 *H* and 1/8 *H* away from the bottom wall in the two struts, respectively (Figure 8a and Figure 8c). The latter design does provide a fuel plume close to the bottom wall. A similar comparison can be made between StrutE-s-2 and StrutE-les-1. Although both the StrutE-le-2 and StrutE-les-1 designs provide a fuel plume near the wall surface, StrutE-les-1 has only one fuel port on the leading edge of the strut, and might be easier to fabricate. In terms of performance, all these designs have similar total pressure recovery, as shown in Figure 9a. StrutE-les-1has higher mixing efficiency near the middle of the strut section, as illustrated in Figure 9b. This design only has one injector port at the leading edge, so that the fuel has more time to mix before the next fuel injection. On the other hand, both StrutE-le-1 and StrutE-le-2 have better mixing efficiency toward the end of the strut. In these cases, all the injector ports are located at the leading edge. As the fuel convects downstream, it has more time to interact with the flow field around the strut surface. Hence, for the cases with all the ports on the side of the strut, *ie.*, StrutE-s-1, StrutE-s-2 and StrutE-st, the mixing efficiency is lower, as shown in Figure 9b. Note that the vertical dash lines represent the starting and ending positions of the strut region, and the locations of the injector ports are denoted by the circular symbols. The performance of the StrutE-les-1 will be considered as a baseline design for the purposes of comparison with other designs.

Placing the first injection port near the bottom wall (StrutE-le-2 and StrutE-les-1) does provide fuel distribution closer to the wall surface. Therefore the next two designs studied have the flush-wall injector, as in StrutE-sw-1 and StrutE-sw-2 (Figure 3g and Figure 3h). The StrutE-sw-1 with the flush-wall injector near the leading edge provides better fuel distribution near the bottom wall and also in the lateral direction, as compared with the StrutE-sw-2, as shown in Figure 10. It also performs better than StrutE-les-1 (Figure 8e). There is no significant difference in terms of total pressure recovery among these three designs, as shown in Figure 11a. In terms of mixing efficiency, however, StrutE-les-1 seems to perform better than the other two designs (StrutE-sw-1 and StrutE-sw-2), as depicted as Figure 11b. The fuel injected from the flush-wall injector mainly travels along the junction between the strut and the bottom wall, where the flow field is dominated by the turbulent boundary layer. On the other hand, for StrutE-les-1, the fuel has a stronger interaction with the flow field on the strut surface due to higher velocity gradient, particularly at the expansion corner between the leading edge and the side of the strut. These flow phenomena can

be observed from the pressure contours. The pressure variations on the wall surface near the strut (Figure 10) are less severe than that observed between the leading edge and the side (Figure 8e).

Strut G and StrutH configurations

Several minor modifications of the StrutE design were tested, looking for better fuel distribution behind the strut, particularly near the bottom wall. Figure 12 shows the flow features for StrutG-le, StrutG-s and StrutH-les. The difference between StrutG-le and StrutG-s is the fueling scheme. StrutG-le has all the fuel ports on the leading edge, while StrutG-s has the injectors on the side. Although StrutH-les appears to offer better lateral fuel spreading near the wall surface (Figure 12), it has higher total pressure loss than the other designs, as illustrated in Figure 13a. This higher loss is mainly caused by the shape of the strut at the trailing edge. StrutE-les-1 (Figure 8e) has the same fuel scheme as StrutH-les -- the only difference between the two is at the trailing edge. StrutE-les-1 has a gradual decrease in total pressure along the strut region. StrutH-les, however, has a sudden drop in the total pressure right after the trailing edge (Figure 13a), which indicates that it creates a larger wake region. Thus it provides better mixing characteristics (Figure 13b). Note that the penetration height of the fuel is not changed by any of the strut designs tested or by the placement of the fuel ports.

Asymmetric StrutE configuration

An asymmetric variation on the StrutE configuration was tested with two different fuel schemes to study their mixing characteristics (Figure 5). As mention earlier due to the asymmetric of the strut design, the computational domain consisted of the whole cross-section area of the isolator, *i.e.*, there is no symmetry assumption at the centerline. Since StrutI-les-1 has only three fuel ports on one side of the strut, the fuel distribution tends to be concentrated on that side as it is convected downstream ($x = 0.9652\ m$), as shown in Figure 14a. With injection ports on both sides of the strut, StrutI-les-2 produces a more uniform spread on both sides, as compared to StrutI-les-1 (Figure 14b). Note that the results for both struts show asymmetric flow distributions downstream of the strut, and, most importantly, a significant amount of fuel concentrated on the bottom wall ($x = 0.9652\ m$). This indicates that there is a strong vortex interaction between the strut and the wall surface. Given that the width of these struts is half that of all the other designs, the total pressure losses for StrutI-les-1 and StrutI-les-2 are lower. A comparison with StrutE-les-1 is shown in Figure 15a. There are two principal reasons for this; first, the strut is half the width, and second, it has is flat surface on one side, and the flat surface does not create as much flow disturbance as the compression and expansion surfaces. Of course, the mixing efficiencies of the StrutI designs are not as good as the StrutE-les-1 design, as depicted in Figure 15b.

Forward-swept strut

Most of the struts studies have a backward-swept angle (Figure 3-Figure 5), which tends to divert the fuel plume upward to the core flow, and an incline, to decouple the fuel distribution from the bottom wall, as represented in Figure 8b. Therefore, a forward-swept strut configuration, StrutJ, was simulated to determine its ability to distribute the fuel to the bottom wall. Figure 16 shows that the fuel is indeed pushed downward to the wall surface, but no fuel is distributed to the core flow, which defeats the original purpose of using the strut to fuel the core flow. Note that this design created two high pressure regions; one between the leading edge and the wall surface, and the other at the corner of the trailing edge and the wall. Severe local heating will be generated in these two regions, and drag will be increased, as suggested by Povinelli.[26] Both the total pressure recovery and mixing efficiency for the forward-swept strut are not as promising as in the backward-swept configurations, as shown in Figure 15a and Figure 15b, respectively.

StrutE-s-2 at Mach 3

Lastly, the StrutE-s-2 configuration was studied for a Mach 3 flow with the same P_0 (344.7 kPa) and T_0 (294 K) as the Mach 2 case. Since the oblique-shock angle generated from the leading edge is smaller for the Mach 3 flow than the Mach 2, the fuel plume is confined in a smaller region behind the strut, as illustrated in Figure 17, as compared to the lower Mach number simulation (Figure 8d). Thus the penetration height is lower, and the fuel is dispersed in a more lateral direction and concentrated along the bottom wall. Note that the legends for the pressure contour are different for the Mach 2 and 3 simulations. The static pressure for Mach 3 is lower, because P_0 was kept the same. Therefore the overall total pressure recovery is much lower for Mach 3, as shown in Figure 18a. Due to

the fact that the fuel is more confined in the higher Mach number case, the mixing efficiency is lower as compared to the Mach 2 flow, as depicted in Figure 18b.

IV. Conclusions

Numerical simulations were performed for struts with various fueling schemes to study their performance in terms of fuel distribution, total pressure recovery and mixing efficiency. A total of fourteen strut-injection designs were tested for the fuel/air mixing characteristics. This study mainly focused on Mach 2 inflow conditions, although one simulation was conducted for a Mach 3 flow. Overall, there is no significant difference in the penetration height of the fuel plume from the various backward-swept strut-injection configurations. Having a fuel port at the tip of the strut, StrutE-st, does not improve the penetration height, because the fuel tends to be pushed downward at the trailing edge due to flow expansion.

Placing one of the fuel ports close to the wall at 1/8 *H*, or having a flush-wall injector, could improve the fuel distribution close to the wall surface for ignition purposes. Although asymmetric StrutE configurations (StrutI-les-1 and StrutI-les-2) can provide fuel close to the wall, their mixing efficiency is not as high as StrutE-les-1. The StrutE-les-1 design is considered to have the best fuel/air mixing flow characteristics and mixing efficiency with the least significant loss in total pressure, as compared to other strut-injection designs.

StrutJ, a forward-swept strut configuration, brings the fuel toward the bottom wall but inhibits fuel distribution to the core flow. This design creates two high pressure regions; one between the leading edge and the wall surface, and the other at the corner of the trailing edge and the wall. The flow phenomena could potentially generate severe local heating in these two regions, and an increase in drag.

The StrutE-s-2 design was tested for both Mach 2 and 3 flow conditions with the same T_0 and P_0. The oblique-shock angle generated from the leading edge is smaller for the Mach 3 case, and therefore the fuel plume is more confined in a smaller region behind the strut. Consequently, the mixing efficiency is poorer for the Mach 3 condition than the Mach 2 flow.

Although the mass flow rate of gaseous ethylene for the current study is relatively small (1.9634×10^{-3} *kg*/*sec*), future work will perform for higher fuel flow rates for larger scale scramjet-combustor designs.

V. Acknowledgments

This study was supported by and performed at Wright-Patterson Air Force Base, under Contract F33615-03-D-2419. The support for this project is sincerely appreciated. Additional support took the form of a grant of computer resources from the ASC, ARL and ERDC Department of Defense High Performance Computing Center. The authors would also like to thank Anna Creese of Taitech for her editorial consultation.

VI. References

1. Fuller, R.P., Wu, P.-K., Kirkendall, K.A., and Nejad, A.S., "Effects of Injection Angle on Atomization of Liquid Jets in Transverse Airflow," *AIAA Journal*, Vol. 38, No. 1, 2000, pp. 64-72.
2. Ali, M. and Sadrul Islam, A.K.M., "Study on Main Flow and Fuel Injector Configurations for Scramjet Applications," *International Journal of Heat and Mass Transfer*, Vol. 49, 2006, pp. 3634–3644.
3. Lewis, D.P. and Schetz, J.A., "Tangential Injection from Overlaid Slots into a Supersonic Stream," *Journal of Propulsion and Power*, Vol. 13, No. 1, 1997, pp. 59-63.
4. Rowan, S.A. and Paull, A., "Performance of a Scramjet Combustor with Combined Normal and Tangential Fuel Injection," AIAA Paper 2005-0615, 2005.
5. Gruber, M.R., Nejad, A.S., Chen, T.H., and Dutton, J.C., "Transverse Injection from Circular and Elliptical Nozzles into a Supersonic Crossflow," *Journal of Propulsion and Power*, Vol. 16, No. 3, 2000, pp. 449-457.
6. Barber, M.J., Schetz, J.A., and Roe, L.A., "Normal, Sonic Helium Injection Through a Wedge-Shaped Orifice into Supersonic Flow," *Journal of Propulsion and Power*, Vol. 13, No. 2, 1997, pp. 257-263.
7. Tomioka, S., Jacobsen, L.S., and Schetz, J.A., "Sonic Injection from Diamond-Shaped Orifices into a Supersonic Crossflow," *Journal of Propulsion and Power*, Vol. 19, No. 1, 2003, pp. 104-114.
8. Grossman, P., Maddalena, L., and. Schetz, J.A., "Wall Injectors for High Mach Number Scramjets," AIAA Paper 2006-4682, 2006.
9. Jacobsen, L.S., Gallimore, S., Schetz, J.A., O'Brien, W., and Goss, L., "Improved Aerodynamic-Ramp Injector in Supersonic Flow," *Journal of Propulsion and Power*, Vol. 19, No. 4, July-August 2003.

10. Lee, S.-H., "Characteristics of Dual Transverse Injection in Scramjet Combustor, Part 2: Combustion," *Journal of Propulsion and Power*, Vol. 22, No. 5, 2006, pp. 1020-1026.
11. Price, B.B., Elliot, G.S., and Ogot, M., "Experimental Optimization of Transverse Jet Injector Geometries for Mixing into a Supersonic Flow," AIAA Paper 1998-3019, 1998.
12. Mathur, T., Cox-Stouffer, S.K., Hsu. K.-Y., Crafton, J., Donbar, J.M., and Gruber, M.R., "Experimental Assessment of a Fuel Injector for Scramjet Applications," AIAA Paper 2000-3703, 2000.
13. Cox-Stouffer, S.K., Gruber, M.R., and Bulman, M.J., "A Streamlined, Pressure-Matched Fuel Injector for Scramjet Applications," AIAA Paper 2000-3707, 2000.
14. Kobayashi, K., Tomioka, S., Kato, K., Murakami, A., and Kudo, K., "Performance of a Dual-Mode Combustor with Multistaged Fuel Injection," *Journal of Propulsion and Power*, Vol. 22, No. 3, 2006, pp. 518-526.
15. Takahashi, S., Sato, N., Tsue, M., Kono, M., Nakamura, M., Kondo, H., and Ujiie, Y., "Control of Flame-Holding in Supersonic Airflow by Secondary Air Injection," *Journal of Propulsion and Power*, Vol. 14, No. 1, 1998, pp. 18-23.
16. Cutler, A.D. and Doerner, S.E., "Effects of Swirl and Skew Upon Supersonic Wall Jet in Crossflow," *Journal of Propulsion and Power*, Vol. 17, No. 6, 2001, pp. 1327-1332.
17. Kawano, S., Aso, S., and Orino, M., "A Study of a New Injector for Improvement of Supersonic Mixing," AIAA Paper 2000-0089, Jan. 2000.
18. Shreenivasan, O., Kumar, R., Kumar, T., Sujith, R., and Chakravarthy, S., "Mixing in Confined Supersonic Flow Past Strut Based Cavity and Ramps," AIAA Paper 2004-4194, 2004.
19. Manoharan, S., Chandra, B., Chakravarthy, S., Ramakrishnan, S., and Subramanyam, J., "Experimental Studies of Supersonic Cold Flow Mixing with Ramp Mixers," *Journal of Aerospace Engineering*, Vol. 18, No. 4, Oct. 2005, pp. 197-205.
20. Hsu, K.-Y., Carter, C., Gruber, M., and Barhorst, T., "Experimental Study of Cavity-Strut Combustion in Supersonic Flow," AIAA Paper 2007-5394, 2007.
21. Doster, J., King, P., Gruber, M., Maple, R., "Pylon Fuel Injector Design for a Scramjet Combustor," AIAA Paper 2007-5404, 2007.
22. Metacomp, http://www.metacomptech.com/index.html, 2006.
23. Gruber, M.R. and Nejad, A.S., "New Supersonic Combustion Research Facility," *Journal of Propulsion and Power*, Vol.11, No.5, 1995, pp.1080-1083.
24. Tam, C.-J., Hsu, K.-Y., Gruber, M.R., and Raffoul, C.N., "Aerodynamic Performance of an Injector Strut for a Round Scramjet Combustor," AIAA Paper, 2007-5403, 2007.
25. Hsu, K., Carter, C., Gruber, M.R., and Barhorst, T., "Experimental Study of Cavity-Strut Combustion in Supersonic Flow," AIAA Paper 2007-5394, 2007.
26. Povinelli, L.A., "Aerodynamic Drag and Fuel Spreading Measurements in a Simulated Scramjet Combustion Module," NASA TN D-7674, 1974.

Table 1 Placements of the injection ports for each side of the strut configurations.

	Leading edge	Side	Tip	Flush-wall injector	Number of ports on the strut
StrutE-le-1	3				6
StrutE-s-1		3			6
StrutE-le-2	3				6
StrutE-s-2		3			6
StrutE-les-1	1	2			6
StrutE-st		3	1		7
StrutE-sw-1		2		1	4
StrutE-sw-2		2		1	4
StrutG-le	3				6
StrutG-s		3			6
StrutH-les	1	2			6
StrutI-les-1‡	1	2			3
StrutI-les-2	1	2			6
StrutJ		3			6

‡ Injection ports on one side of the strut only.

le leading edge of the strut
s side wall of the strut
t tip of the strut
w flush-wall injector

les leading edge + side
st side + tip
sw side + wall

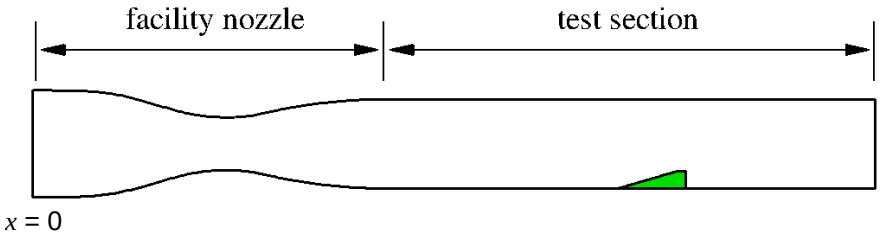

Figure 1 Schematic of AFRL/RZA RC 19 supersonic wind-tunnel facility and strut location.

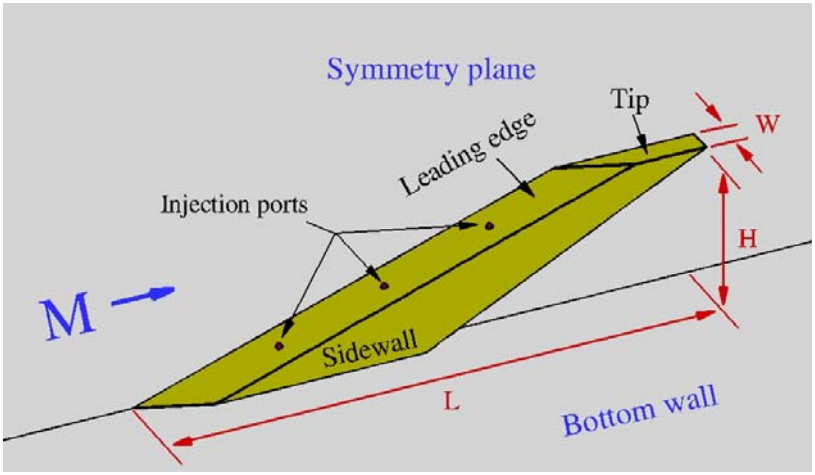

Figure 2 Sketch of the strut with injection ports.

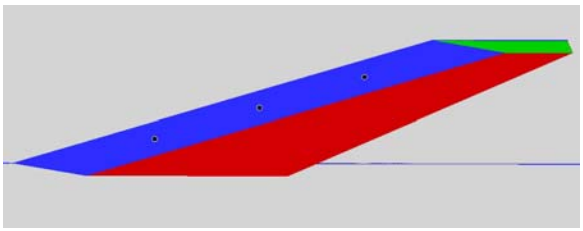

(a) StrutE-le-1

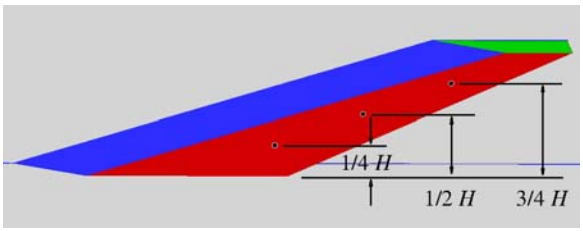

(b) StrutE-s-1

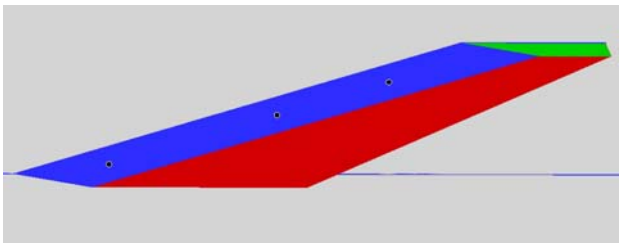

(c) StrutE-le-2

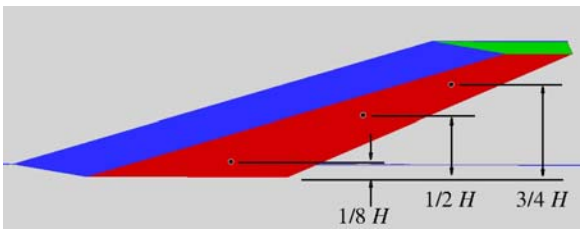

(d) StrutE-s-2

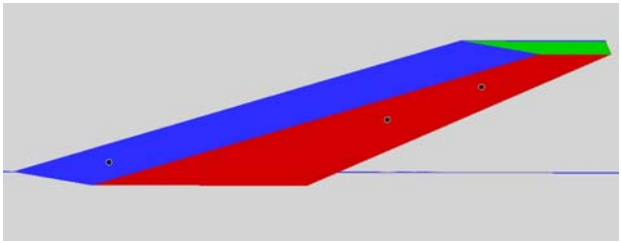

(e) StrutE-les-1

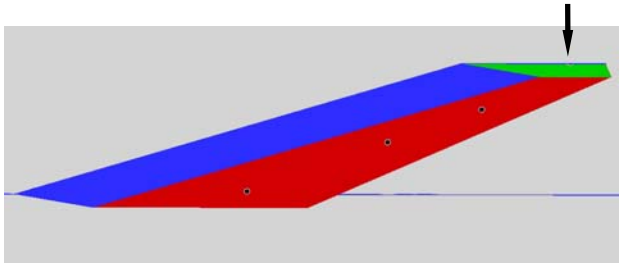

(f) StrutE-st, injector at the tip

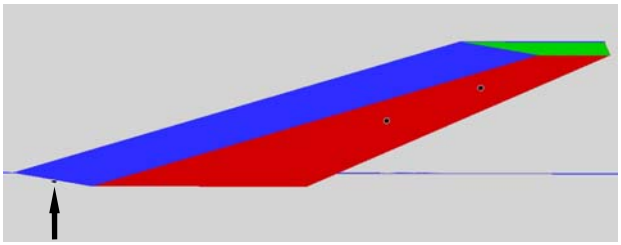

(g) StrutE-sw-1, flush-wall injector near the leading edge

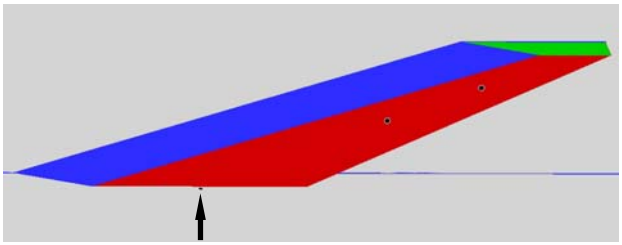

(h) StrutE-sw-2, flush-wall injector near the side

Figure 3 Various fueling schemes for StrutE configuration.

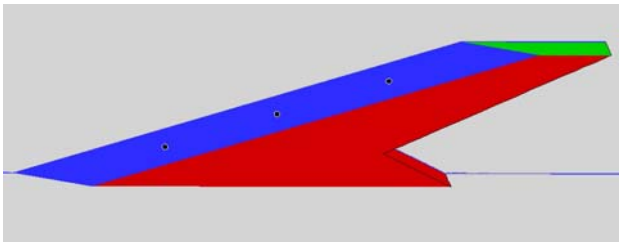

(a) StrutG-le

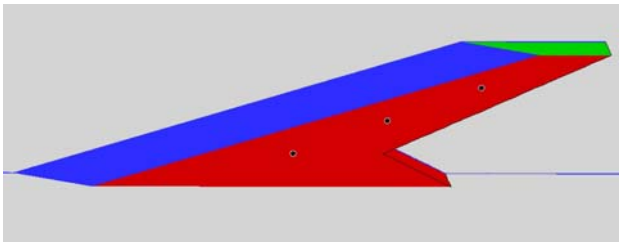

(b) StrutG-s

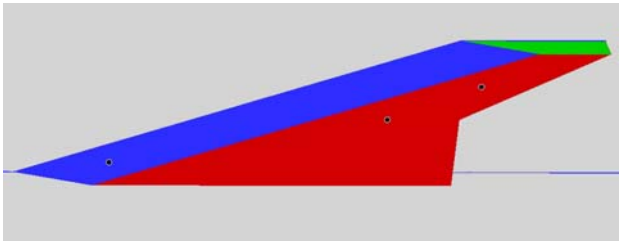

(c) StrutH-les

Figure 4 Modifications of StrutE with different fueling schemes.

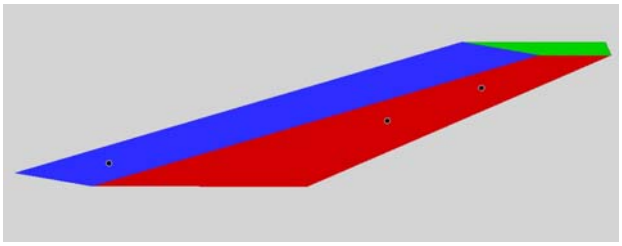

(a) StrutI-les-1, fuel-injection ports on one side

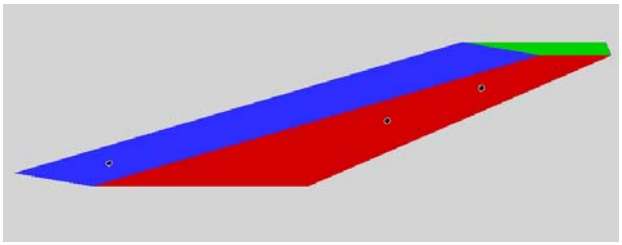

(b) StrutI-les-2, fuel-injector ports on both sides

Figure 5 Asymmetric StrutE configuration with flat surface on opposite side.

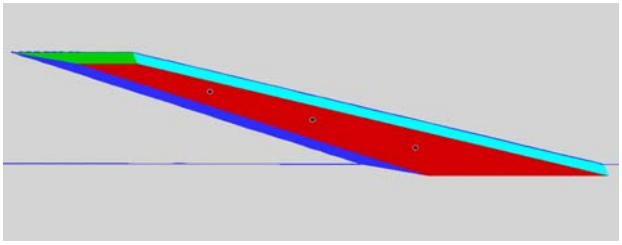

Figure 6 StrutJ, forward-swept strut configuration.

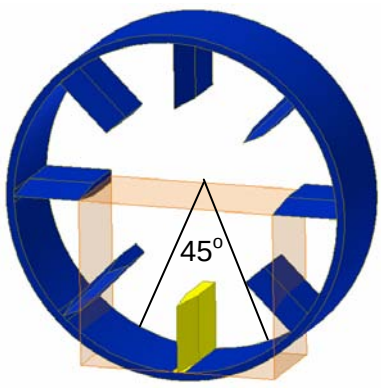

Figure 7 A single strut in a 12.7 *cm* x 15.24 *cm* rectangular flow path with overlay of 25.4 *cm* round combustor with eight-strut injection.

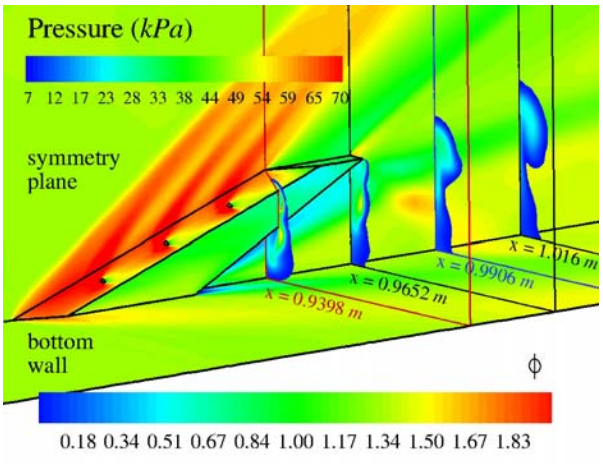

(a) StrutE-le-1

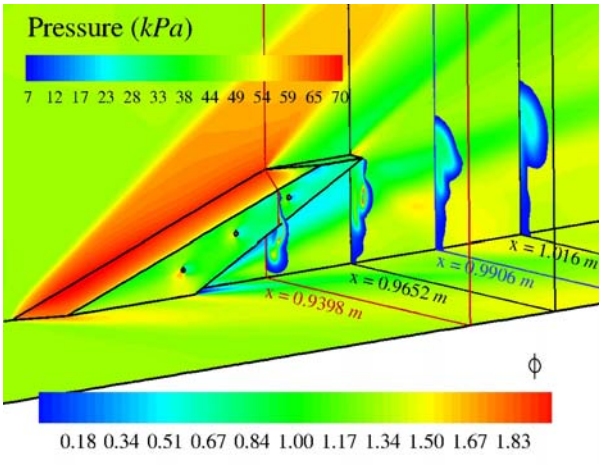

(b) StrutE-s-1

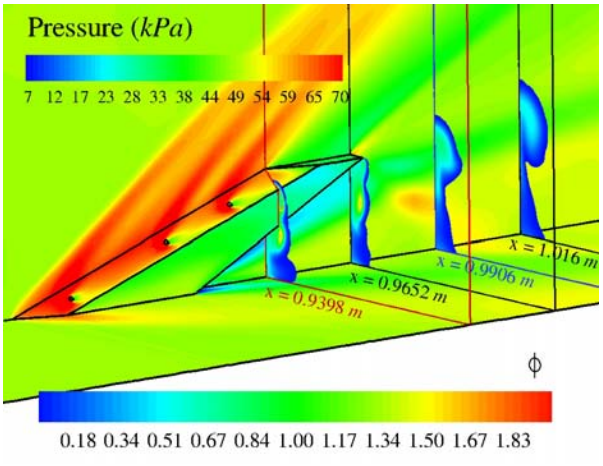

(c) StrutE-le-2

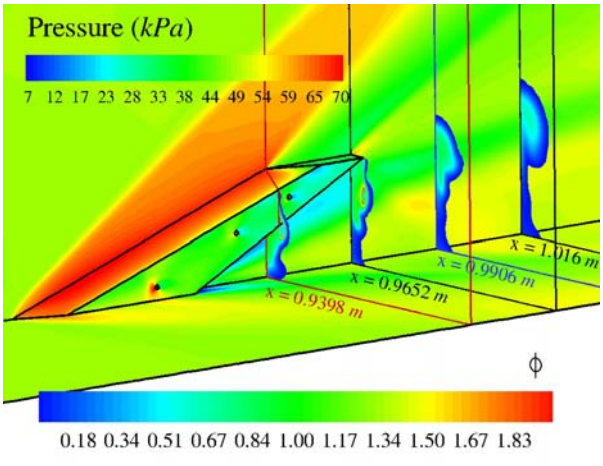

(d) StrutE-s-2

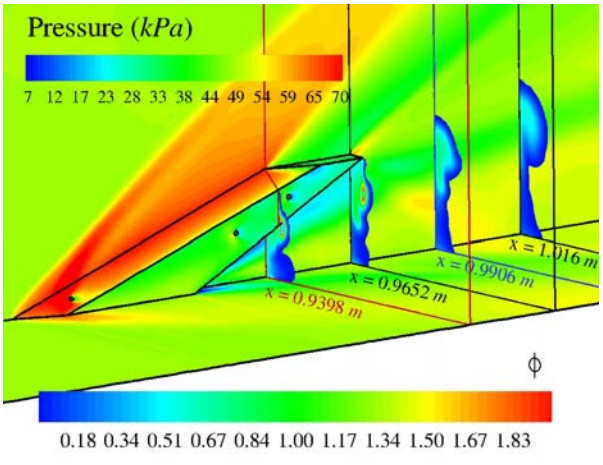

(e) StrutE-les-1

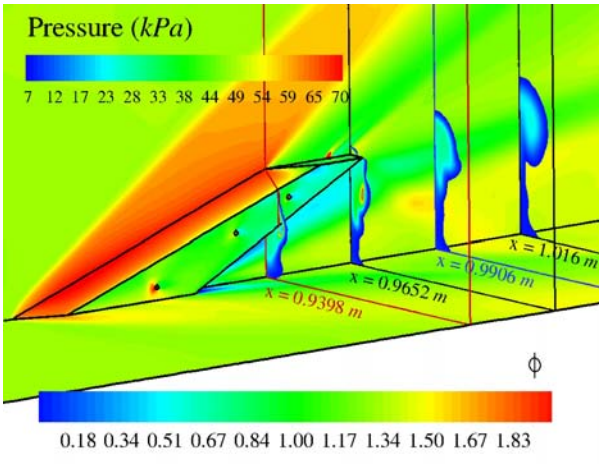

(f) StrutE-st

Figure 8 Contours of static pressure and φ for various fueling schemes with StrutE configuration.

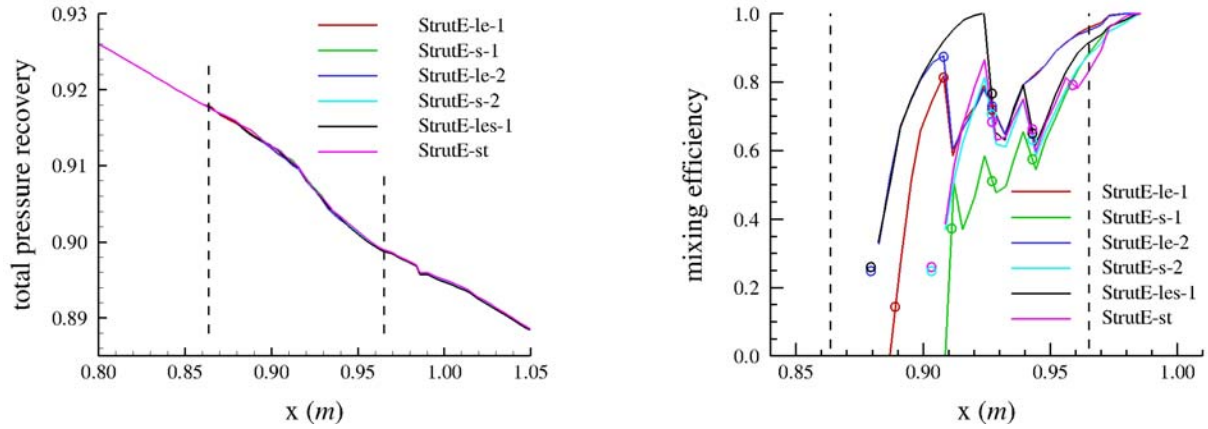

(a) Total pressure recovery (b) Mixing efficiency

Figure 9 1-D performance analysis for various StrutE fueling schemes.

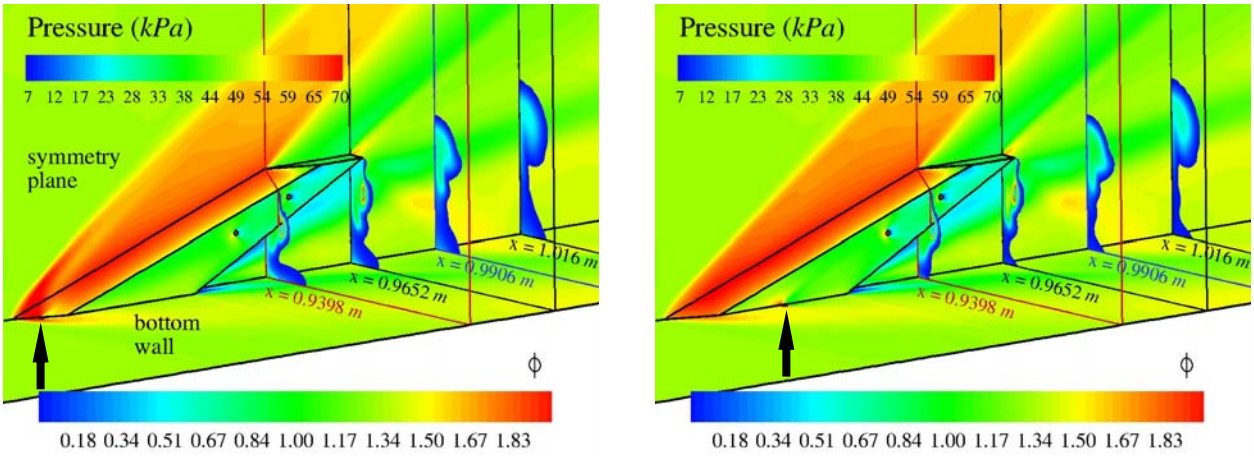

(a) StrutE-sw-1, flush-wall injector near the leading edge (b) StrutE-sw-2, flush-wall injector near the side

Figure 10 Contours of static pressure and φ for StrutE configuration with flush-wall injectors.

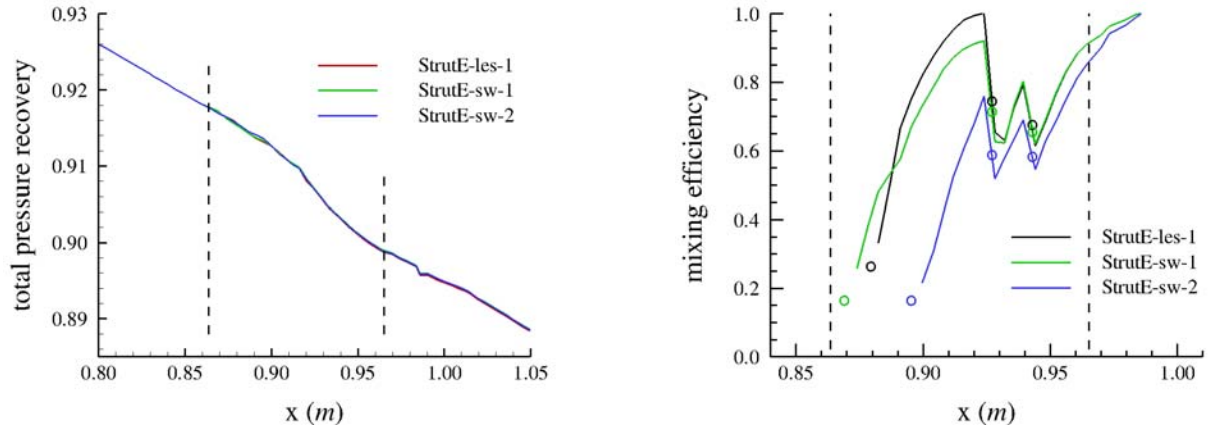

(a) Total pressure recovery (b) Mixing efficiency

Figure 11 1-D performance analysis for StrutE with flush-wall injectors.

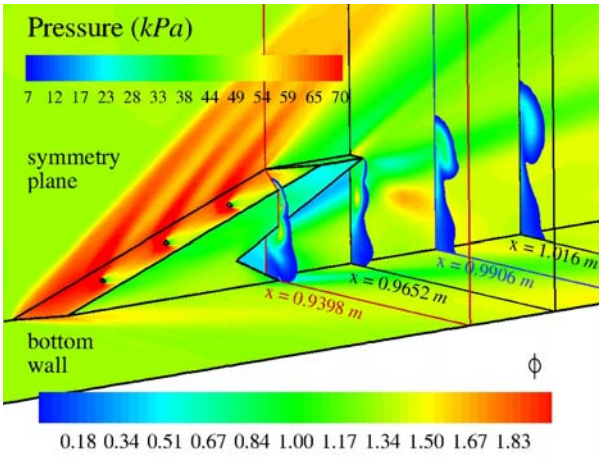

(a) StrutG-le

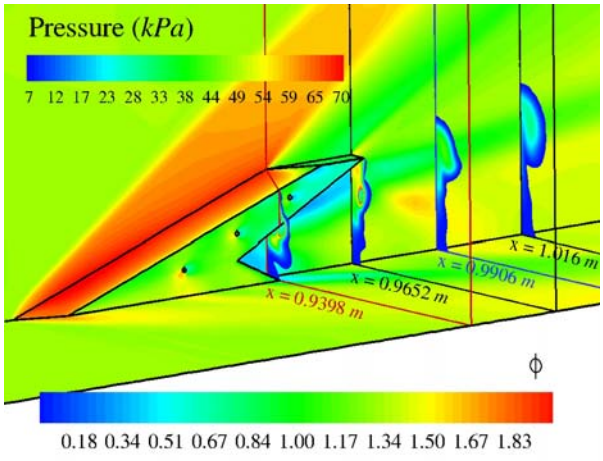

(b) StrutG-s

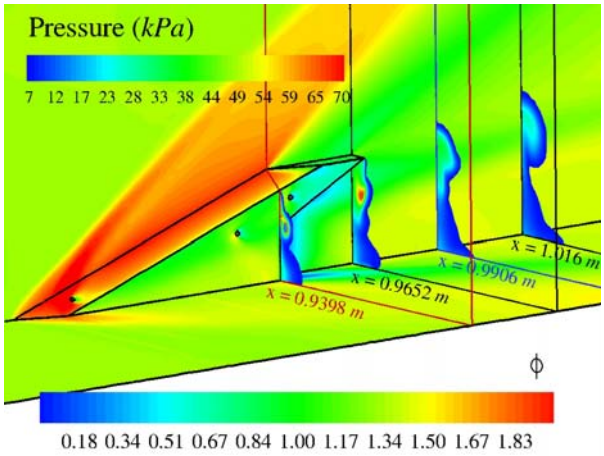

(c) StrutH-les

Figure 12 Contours of static pressure and φ for StrutG and StrutH configurations.

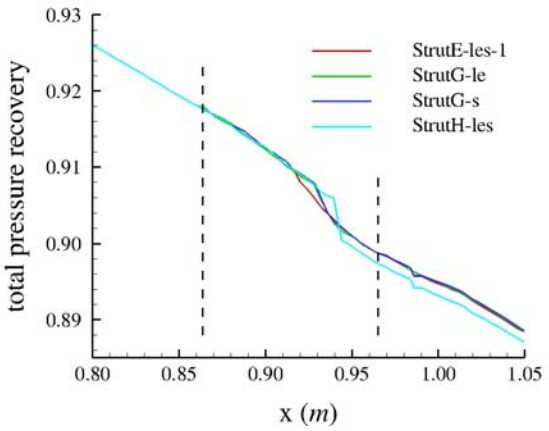

(a) Total pressure recovery

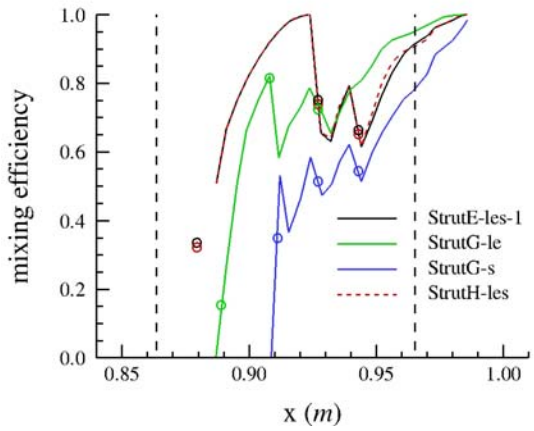

(b) Mixing efficiency

Figure 13 1-D performance analysis for StrutG and StrutH configurations.

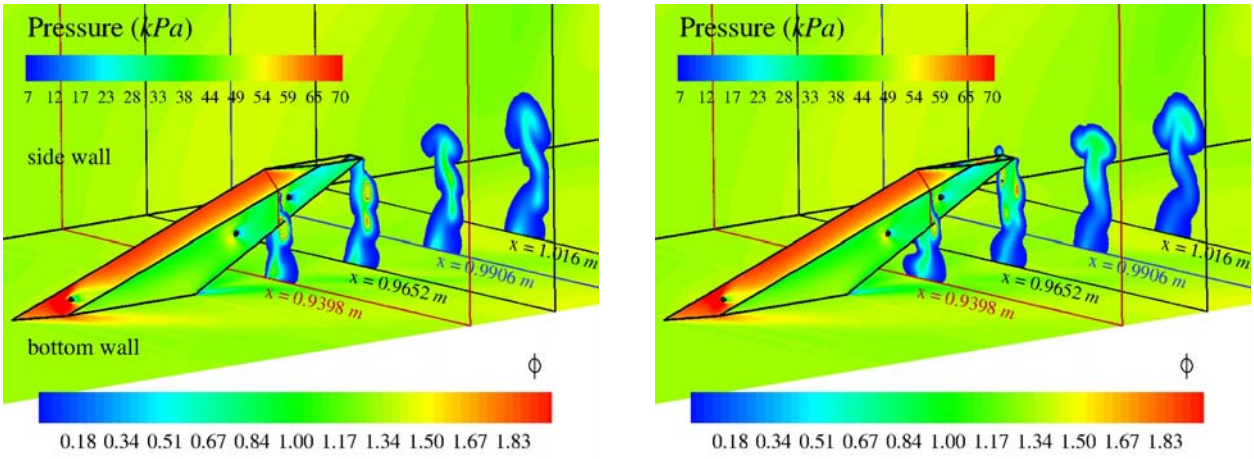

(a) Fuel-injection ports on one side, StrutI-les-1 (b) Fuel-injector ports on both sides, StrutI-les-2

Figure 14 Contours of static pressure and φ for StrutI configuration with flat surface on opposite side.

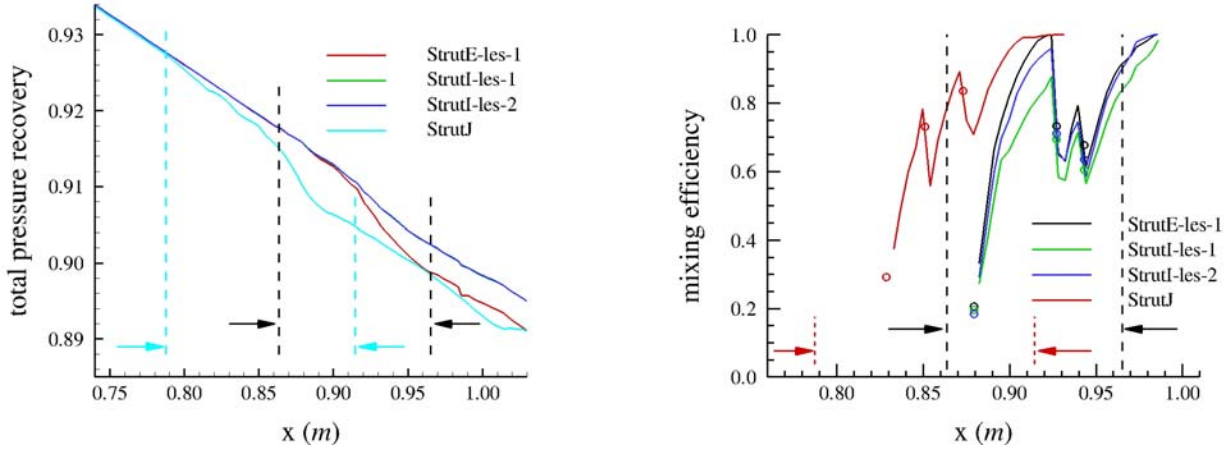

(a) Total pressure recovery (b) Mixing efficiency

Figure 15 1-D performance analysis for asymmetric StrutI and StrutJ configurations.

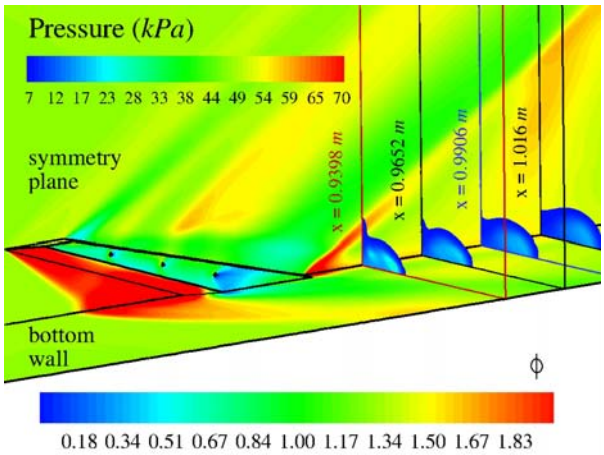

Figure 16 Contours of static pressure and φ for forward-swept strut configuration, StrutJ.

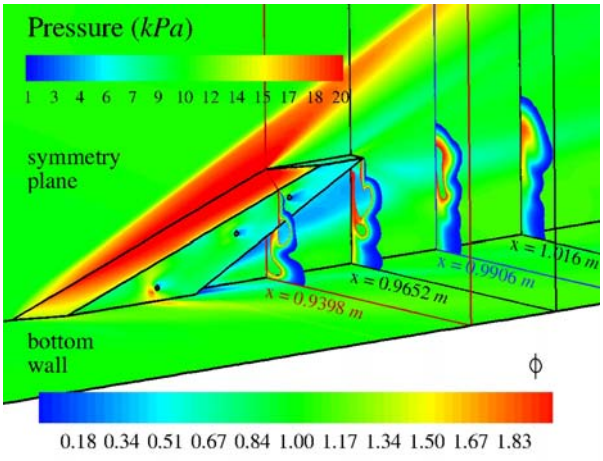

Figure 17 StrutE-s-2 configuration at Mach 3.

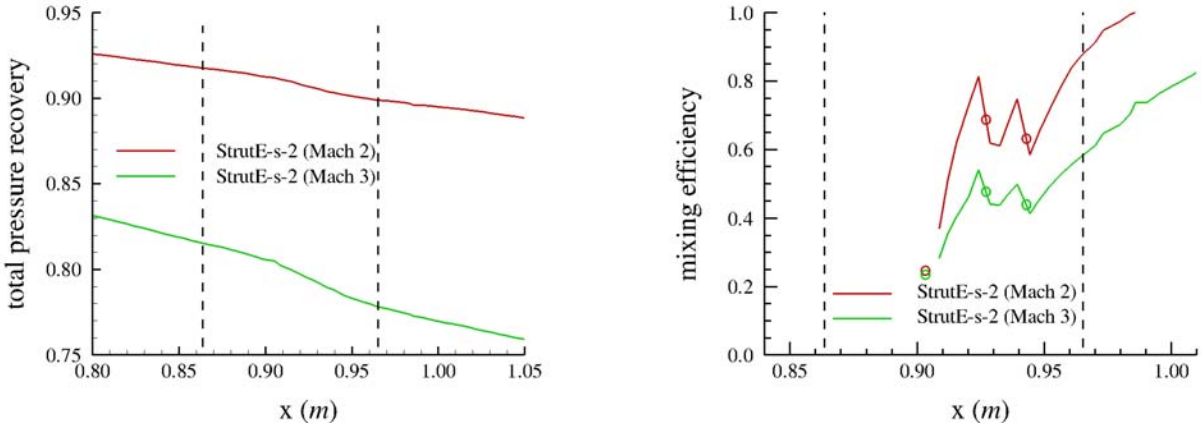

(a) Total pressure recovery (b) Mixing efficiency

Figure 18 1-D performance analysis for StrutE-s-2 configuration at Mach 2 and 3 flight conditions.